dium in the product was 3.04 ± 0.02, and the X-ray diffraction pattern was NASICON-like (Figure 1e), indicating that hydrogen insertion had indeed occurred.[8] The product could therefore be formulated as $H_3V_2(PO_4)_3$. We could not prepare $H_3V_2(PO_4)_3$ from $Na_3V_2(PO_4)_3$ by ion exchange because the latter dissolves in aqueous acids to give green solutions.

In summary, we have synthesized a new vanadium phosphate, $V_2(PO_4)_3$, that poossesses a NASICON-like structure, by oxidatively deintercalating sodium from $Na_3V_2(PO_4)_3$ using chlorine in $CHCl_3$ at room temperature. We have also shown that $V_2(PO_4)_3$ serves as a host material for reductive insertion of lithium and hydrogen under mild experimental conditions.

Acknowledgment. We thank the Department of Science and Technology, Government of India for support of this research.

(8) To find out whether hydrogen is inserted into or oxygen removed from $V_2(PO_4)_3$ during treatment with H_2 at 200 °C, we have recorded the IR spectrum of $H_3V_2(PO_4)_3$ and compared it with the spectra of $Na_3V_2(PO_4)_3$ and $V_2(PO_4)_3$. The spectra of all the compounds are similar (NASICON-like), showing characteristic absorption bands due to PO_4. If oxygen were removed during hydrogen treatment, the framework would have changed considerably, and this would have manifested in the IR spectrum. Moreover, it is known that in oxides such as WO_3 and $LaNiO_3$, hydrogen is inserted into the host rather than oxygen removed under similar experimental conditions.

Chemical Vapor Deposition of Thin Films of Ruthenium and Formation of an Unexpected Byproduct Using Hexafluoro-2-butynetetracarbonylruthenium(0)

Yoshihide Senzaki,† Fred B. McCormick,‡ and Wayne L. Gladfelter*,†

Department of Chemistry, University of Minnesota Minneapolis, Minnesota 55455 and 3M Corporate Research Laboratory St. Paul, Minnesota 55144

Received April 27, 1992
Revised Manuscript Received May 27, 1992

Metallic ruthenium exhibits several physical and chemical properties that make it interesting for applications in the electronics industry.[1] In addition to its metallic conductivity, it is both mechanically strong and chemically inert. Of further interest is the observation that ruthenium oxides (which form on the surface of ruthenium upon exposure to air) exhibit electrical conductivity similar to that of the metal.[2,3] This had led to some interest in using ruthenium as a contact material or diffusion barrier in devices.[4] Earlier work on the chemical vapor deposition of ruthenium utilized $Ru(acac)_3$,[4-6] $Ru_3(CO)_{12}$,[4] and $(\eta^5\text{-}C_5H_5)_2Ru$[4,7] to produce either ruthenium or ruthenium oxide films, depending on the carrier gas. The purest metallic films were prepared from $Ru_3(CO)_{12}$,[4] which has a relatively low vapor pressure. Unfortunately, the more volatile alternative, $Ru(CO)_5$, has a low stability which limits its use as a precursor.

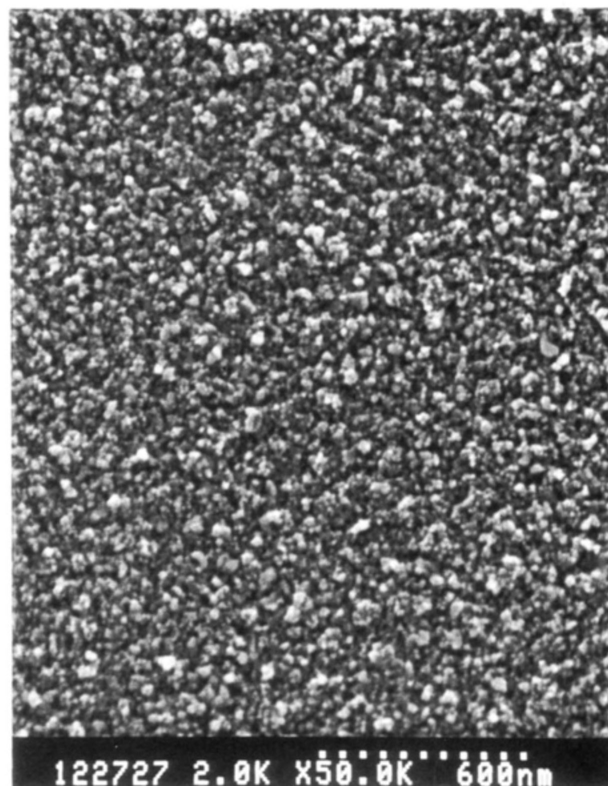

Figure 1. Scanning electron micrograph of a Ru film prepared at 500 °C using $Ru(hfb)(CO)_4$. The scale (600-nm total length) is located in the lower right-hand corner of the Figure.

Gagné and Takats recently reported[8] the synthesis of a series of monometallic alkyne carbonyl complexes of ruthenium, including $Ru(hfb)(CO)_4$, where hfb = hexafluoro-2-butyne, 1. Considering the often observed en-

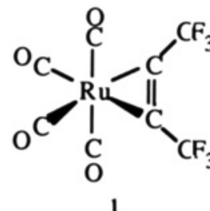

hancement in volatility that fluorine substituents impart to compounds, we initiated a study of the CVD of ruthenium using $Ru(hfb)(CO)_4$. The compound was found to have a vapor pressure between 1 and 2 Torr at room temperature.

The growth of Ru films was conducted without a carrier gas under a dynamic vacuum of approximately 1 mTorr in a hot-wall quartz reactor. The substrates, Si(100) wafers, were placed at several locations toward the entrance to the reactor. A profile of the furnace with the deposition tube present established that a reasonably constant temperature was achieved 2–3 cm from the beginning edge of the heating coils. The substrates were located at the beginning of the constant-temperature re-

† University of Minnesota.
‡ 3M Corporate Research Laboratory.

(1) Green, M. L.; Levy, R. A. *J. Met.* **1985**, *37* (6), 63.
(2) Vadimsky, R. G.; Frankenthal, R. P.; Thompson, D. E. *J. Electrochem. Soc.* **1979**, *126*, 2017.
(3) Rolison, D. R.; Kuo, K.; Umana, M.; Brundage, D.; Murray, R. W. *J. Electrochem. Soc.* **1979**, *126*, 407.
(4) Green, M. L.; Gross, M. E.; Papa, L. E.; Schnoes, K. J.; Brasen, D. *J. Electrochem. Soc.* **1985**, *132*, 2677.
(5) Viguié, J. C.; Spitz, J. *J. Electrochem. Soc.* **1975**, *122*, 585.
(6) Crosby, J. N.; Hanley, R. S. U.S. Patent 4,250,210, 1981.
(7) Trent, D. E.; Paris, B.; Krause, H. H. *Inorg. Chem.* **1964**, *3*, 1057.
(8) Gagné, M. R.; Takats, J. *Organometallics* **1988**, *7*, 561.

0897-4756/92/2804-0747$03.00/0 © 1992 American Chemical Society

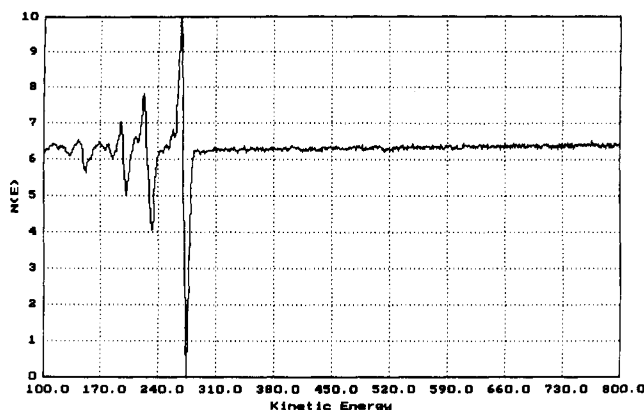

Figure 2. Auger electron spectrum of a Ru film prepared at 500 °C using $Ru(hfb)(CO)_4$.

gion. The relative accuracy of the temperatures reported is estimated to be 5%. At 500 °C, exposure of the wafers to $Ru(hfb)(CO)_4$ for 3 min produced a film having a thickness of 1800 Å as measured by stylus profilometry.

The films were smooth and highly reflective to visual inspection and had a color nearly identical to that of the silicon substrate. Examination of the surface using scanning electron microscopy (SEM) revealed that the grain size of the smooth surface was 300 Å. Close examination of Figure 1 suggests that the film does not exhibit a densely packed microstructure. After sputtering through the top layer of a film grown at 500 °C, a survey Auger electron spectrum (Figure 2) showed no signals attributable to carbon, oxygen, or fluorine. Slower scans over the regions of interest revealed an oxygen content of 1%. Due to the overlap between the carbon KLL line at 271 eV and the ruthenium MNN line at 273 eV, a direct measure of the carbon content was not possible. In previous studies, a comparison of the difference in the intensities of the ruthenium transitions located at 273 and 231 eV relative to ruthenium standards was used as a gauge of the carbon content.[4] In pure ruthenium, the value of I_{273}/I_{231} was 2.64. In the films grown using $Ru(hfb)(CO)_4$ the observed ratio of 2.64 indicated that the carbon content was below the limits of detection. Alternative methods for carbon analysis are being explored. X-ray diffraction of the films established that they were polycrystalline with no preferential orientation. Measurement of the resistivity of the films (four-point probe) gave a value of 160 $\mu\Omega$ cm, which compares to the resistivity of bulk ruthenium of 7.6 $\mu\Omega$ cm.[9] The higher value may be due to the porous microstructure suggested from the SEM analysis or to carbon impurities not detected by the above procedure.

When the temperature of the deposition was lowered to 300 °C, the thickness of the film was notably decreased and a yellow crystalline solid was observed at both the entrance and exit of the reactor. By 150 °C, no film deposition occurred and a larger quantity of the yellow solid was isolated. The new compound, **2**, was completely characterizing using analytical and spectroscopic methods[10]

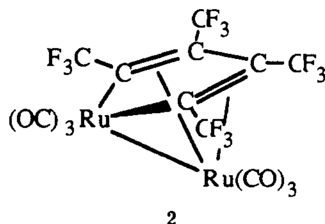

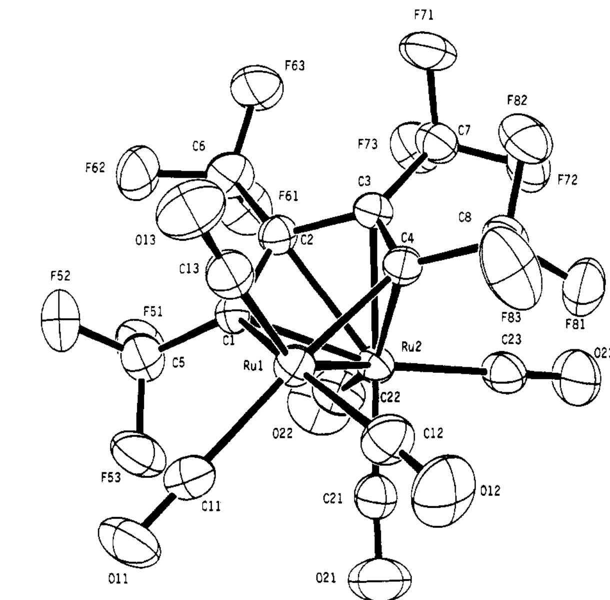

Figure 3. Molecular structure of $Ru_2[\mu\text{-}\eta^1{:}\eta^1{:}\eta^4\text{-}C_4(CF_3)_4](CO)_6$ with thermal ellipsoids shown at the 50% level. Selected bond distances (Å): Ru1–Ru2 = 2.7589 (7), Ru1–C1 = 2.073 (4), Ru1–C4 = 2.069 (4), C1–C2 = 1.420 (6), C2–C3 = 1.444 (6), C3–C4 = 1.437 (6), Ru2–C1 = 2.223 (4), Ru2–C2 = 2.278 (4), Ru2–C3 = 2.227 (4), Ru2–C4 = 2.259 (4).

and, ultimately, by single-crystal X-ray crystallography.[11] The structure of $Ru_2[\mu\text{-}\eta^1{:}\eta^1{:}\eta^4\text{-}C_4(CF_3)_4](CO)_6$, Figure 3, results from loss of CO and coupling of the alkyne ligands from 2 equiv of $Ru(hfb)(CO)_4$. Within the iron triad numerous examples of this structural type are known.[12] The surprisingly high yields (47% at 300 °C; 72% at 150 °C) formed during this flash vacuum pyrolysis are a testament to the stability of this dimer. Although its volatility was significantly less than that $Ru(hfb)(CO)_4$, ruthenium films could be prepared at 500 °C using $Ru_2[\mu\text{-}\eta^1{:}\eta^1{:}\eta^4\text{-}C_4(CF_3)_4](CO)_6$ as the precursor (the precursor vessel was heated to 70 °C). The dimer can also be synthesized by heating a toluene solution of $Ru(hfb)(CO)_4$ to reflux for 3 h.

The observation that this chemistry occurs equally well both in toluene solution (where surface effects should be minimized) and in the vacuum pyrolysis suggests that the initial chemistry (eq 1) in the CVD process takes place in

$$Ru(hfb)(CO)_4 \rightarrow Ru(hfb)(CO)_3 + CO \quad (1)$$

the gas phase. At temperatures where $Ru(hfb)(CO)_3$ has a long enough lifetime to collide with another complex, presumably $Ru(hfb)(CO)_4$, formation of the dimer may predominate (eq 2). At higher temperatures further ligand

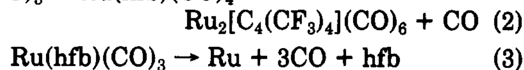

$$Ru(hfb)(CO)_3 + Ru(hfb)(CO)_4 \rightarrow Ru_2[C_4(CF_3)_4](CO)_6 + CO \quad (2)$$

$$Ru(hfb)(CO)_3 \rightarrow Ru + 3CO + hfb \quad (3)$$

(9) Emsley, J. *The Elements*; Clarendon Press: Oxford, 1989.

(10) Spectroscopic data for $Ru_2[\mu\text{-}\eta^1{:}\eta^1{:}\eta^4\text{-}C_4(CF_3)_4](CO)_6$: IR ($cm^{-1}$, pentane) 2117 (m), 2096 (s), 2064 (s), 2054 (s), 2037 (s), 2021 (w); ^{19}F NMR (ppm from $CFCl_3$, CD_2Cl_2) −45.2 (br s, 6 F), −51.1 (br s, 6 F); ^{13}C NMR (ppm, CD_2Cl_2) 121.6 (q, J_{C-F} = 280.8 Hz), 126.5 (q, J_{C-F} = 274.6 Hz), 138.8 (s), 139.3 (s), 189.9–190.5 (br carbonyl resonances). Anal. Calcd: C, 24.22; H, 0.00: Found C, 24.23; H, <0.05. EI-MS (*m/e*) 696 (parent ion) followed by fragments corresponding to loss of 6 CO ligands. Melting point 139–140 °C.

(11) X-ray diffraction data for $Ru_2[\mu\text{-}\eta^1{:}\eta^1{:}\eta^4\text{-}C_4(CF_3)_4](CO)_6$: FW 694.27; ρ_{calcd} = 2.460 g cm^{-3}; crystal system = orthorhombic; space group = *Pbca* (No. 61); *T* = 22 °C; *a* = 13.737 (4) Å, *b* = 13.806 (4) Å, *c* = 19.764 (5) Å, *V* = 3748 (3) $Å^3$; *Z* = 8, μ = 17.27 cm^{-1} (empirical correction applied); radiation = Mo Kα; scan range = $0 < 2\Theta < 52°$; unique reflections collected = 4110; reflections used ($I > 2.0\sigma(I)$) = 2940; *R* = 0.033; R_w = 0.040; goodness of fit = 1.14.

(12) Nesmeyanov, A. N.; Rybinskaya, M. I.; Rybin, L. V.; Kaganovich, V. S. *J. Organomet. Chem.* **1973**, *47*, 1.

loss from Ru(hfb)$(CO)_3$ (eq 3) will become increasingly competitive leading to metallic films of ruthenium. Trapping the volatile CVD byproducts was accomplished using a liquid nitrogen cooled U-tube filled with glass beads. The products were distilled into a NMR tube which was sealed under vacuum. After obtaining a ^{19}F NMR spectrum, the contents of the tube were further analyzed using GC-MS-FTIR. These methods established that the majority of the material was hexafluoro-2-butyne. The gas chromatogram showed the elution of two smaller, less well-resolved peaks immediately following the elution of hfb. The highest mass values for these two peaks were m/e = 362 and 324, respectively. These values and the associated fragmentation patterns correspond to the formulas C_8F_{14} and C_8F_{12}. Although it is tempting to attribute the formation of these fluorocarbons to deposition originating from $Ru_2[\mu-\eta^1:\eta^1:\eta^4-C_4(CF_3)_4](CO)_6$, additional studies are required to verify or refute this supposition.

In summary, Ru(hfb)$(CO)_4$ has sufficient volatility to be used in standard CVD equipment. It was found to give smooth, adherent films of metallic ruthenium on Si(100) at 500 °C. At lower temperatures, a new dinuclear ruthenium complex, $Ru_2[\mu-\eta^1:\eta^1:\eta^4-C_4(CF_3)_4](CO)_6$, was isolated during the chemical vapor deposition. Comparison of the gas-phase and solution synthesis of this dimer has yielded some clues regarding the mechanism of the CVD itself.

Acknowledgment. This work was funded by the Center for Interfacial Engineering, a NSF Engineering Research Center, and the Graduate School of the University of Minnesota. We thank Dr. Jeffrey J. Payne (3M) for obtaining the scanning electron micrographs and Dr. Stanley F. Tead (3M) for assistance with the stylus profilometry.

Supplementary Material Available: Complete list of crystallographic data, atom positions and thermal parameters, and bond distances and angles (9 pages); list of structure factors (20 pages). Ordering information is listed on any current masthead page.

Supercritical Fluid Transport–Chemical Deposition of Films

Brian N. Hansen, Brooks M. Hybertson, Robert M. Barkley, and Robert E. Sievers*

Department of Chemistry and Biochemistry and Cooperative Institute for Research in Environmental Sciences University of Colorado Boulder, Colorado 80309-0216

Received September 9, 1991
Revised Manuscript Received May 22, 1992

There are many chemical vapor deposition (CVD) techniques available that can be used for the formation of thin films on a substrate surface. One of the major limitations of CVD methods, however, is that volatile precursor compounds are required. Furthermore, the deposition of mixed-metal compositions by CVD usually requires more than one precursor chamber, and the delivery rates of each of the reagents must be simultaneously controlled to maintain the correct stoichiometric ratio. The preparation of $YBa_2Cu_3O_{7-x}$ films by metal–organic chemical vapor deposition (MOCVD), for example, has been shown to require separate, individually temperature- and carrier-flow-rate-controlled reservoirs for the Y, Ba, and Cu precursor compounds.[1–4] Supercritical fluid transport–chemical deposition (SFT–CD) is a new film deposition technique which can utilize nonvolatile precursors.[5–8] In the SFT–CD process, precursor reagent(s) are dissolved in a supercritical fluid in a single reservoir, and then this solution, under high pressure, passes through a restrictor into a deposition chamber where the rapid expansion of the supercritical fluid causes vaporization of the solute(s). The vaporized precursor compounds are then induced to react at or near a substrate surface to form a thin film.[5,6] This new process has some important advantages over CVD. Unlike CVD processes, it is not necessary for the precursors to be volatile. When the high-pressure supercritical fluid solution is allowed to expand rapidly into a region of much lower pressure, the solute compounds form very small molecular clusters, ion pairs, or dispersed individual molecules.[9–11] If aerosols rather than vapors are formed, the aerosol particles are much smaller than those formed by the nebulization of ordinary liquid solutions followed by desolvation,[9] such as in spray pyrolysis.

Supercritical fluid solutions have previously been used in purely physical processes for the formation of thin films and fine powders.[10–14] However, this physical deposition method has the disadvantage that the film to be formed must be soluble in the supercritical fluid, because the deposit is chemically identical to the starting material. Many desirable materials, e.g., semiconductors, metals, metal oxides, and mixed-metal oxides, are insoluble in common supercritical fluids such as CO_2 and N_2O. SiO_2 and GeO_2 have been shown to be soluble in supercritical water, but the experimental conditions were rather extreme (445 °C, 8400 psi).[13] The SFT–CD process is distinctly different from the previously described physical process

(1) Berry, A. D.; Gaskill, D. K.; Holm, R. T.; Cukauskas, E. J.; Kaplan, R.; Henry, R. L. Formation of high T_c superconducting films by organometallic chemical vapor deposition. *Appl. Phys. Lett.* **1988**, *52*, 1743.
(2) Zhao, J.; Dahmen, K.-H.; Marcy, H. O.; Tonge, L. M.; Marks, T. J.; Wessels, B. W.; Kannewurf, C. R. Organometallic Chemical Vapor Deposition of High T_c Superconducting Films Using a Volatile, Fluorocarbon-Based Precursor. *Appl. Phys. Lett.* **1988**, *53*, 1750.
(3) Dickinson, P. H.; Geballe, T. H.; Sanjuro, A.; Hildenbrand, D.; Craig, G.; Zisk, M.; Collman, J.; Banning, S. A.; Sievers, R. E. Chemical Vapor Deposition of YBCO Superconducting Films. *J. Appl. Phys.* **1989**, *66*, 444.
(4) Yamane, H.; Masumoto, H.; Hirai, T.; Isasaki, H.; Watanabe, K.; Kobayashi, N.; Muto, Y.; Kurosawa, H. Y-Ba-Cu-O Superconducting Films Prepared on $SrTiO_3$ Substrates by Chemical Vapor Deposition. *Appl. Phys. Lett.* **1988**, *53*, 1548.
(5) Sievers, R. E.; Hansen, B. N. Chemical Deposition Methods Using Supercritical Fluid Solutions. U.S. Patent 4,970,093, Nov 1990.
(6) Hybertson, B. M.; Hansen, B. N.; Barkley, R. M.; Sievers, R. E. Deposition of Palladium Films by a Novel Supercritical Fluid Transport-Chemical Deposition Process. *Mater. Res. Bull.* **1991**, *26*, 1127.
(7) Hybertson, B. M. Use of Supercritical Fluid Expansion Processes for Drug Delivery, Particle Synthesis, and Thin Film Deposition. Ph.D. Dissertation, University of Colorado, 1991.
(8) Hansen, B. N. Reaction of Aerosols Formed by Supercritical Fluid Expansion. Ph.D. Dissertation, University of Colorado, 1991.
(9) Smith, R. D.; Udseth, H. R. Mass Spectrometry with Direct Supercritical Fluid Injection. *Anal. Chem.* **1983**, *55*, 2266.
(10) Smith, R. D. Supercritical Fluid Molecular Spray Film Deposition and Powder Formation. U.S. Patent 4,582,731, Apr 1986.
(11) Smith, R. D. Supercritical Fluid Molecular Spray Thin Films and Fine Powders. U.S. Patent 4,734,451, Mar 1988.
(12) Smith, R. D. Method of Making Supercritical Fluid Molecular Spray Films, Powder and Fibers. U.S. Patent 4,734,227, Mar 1988.
(13) Matson, D. W.; Fulton, J. L.; Petersen, R. C.; Smith, R. D. Rapid Expansion of Supercritical Fluid Solutions: Solute Formation of Powders, Thin Films, and Fibers. *Ind. Eng. Chem. Res.* **1987**, *26*, 2298.
(14) Tom, J. W.; Debenedetti, P. G. Particle Formation with Supercritical Fluids—A Review. *J. Aerosol Sci.* **1991**, *22*, 555.

0897-4756/92/2804-0749$03.00/0 © 1992 American Chemical Society